# Squalene Synthase: Steady-State, Pre-Steady-State, and Isotope-Trapping Studies†

Evette S. Radisky‡ and C. Dale Poulter*

*Department of Chemistry, University of Utah, Salt Lake City, Utah 84112*

*Received June 29, 1999; Revised Manuscript Received November 15, 1999*

ABSTRACT: Squalene synthase catalyzes two consecutive reactions in sterol biosynthesis—the condensation of two molecules of farnesyl diphosphate (FPP) to form the cyclopropylcarbinyl intermediate presqualene diphosphate (PSPP) and the subsequent rearrangement and reduction of PSPP to form squalene. Steady-state and pre-steady-state kinetic studies, in combination with isotope-trapping experiments of enzyme•substrate complexes, indicate that two molecules of FPP add to the enzyme before NADPH and that PSPP is converted directly to squalene without dissociating from the enzyme under normal catalytic conditions. In addition, formation of PSPP or a prior conformational change in squalene synthase is the rate-limiting step for synthesis of squalene from FPP via PSPP in the presence of NADPH and for synthesis of PSPP in the absence of NADPH. Squalene synthase is inhibited at high concentrations of FPP. Inhibition is specific for the formation of squalene, but not PSPP, and is competitive with respect to NADPH. In addition, the binding of either NADPH or a third, nonreacting molecule of FPP stimulates the rate of PSPP formation. A kinetic mechanism is proposed to account for these observations.

Squalene synthase (EC 2.5.1.21) catalyzes the first two pathway-specific reactions in the biosynthesis of sterols. As illustrated in Scheme 1, the enzyme mediates the condensation of two molecules of farnesyl diphosphate (FPP)[1] to form a c1′-2-3-linked intermediate, presqualene diphosphate (PSPP), and the subsequent rearrangement and reduction of PSPP, with NADPH as a hydride donor, to produce squalene (*1*, *2*). Squalene synthase is localized in the membrane of the smooth endoplasmic reticulum (*3*) and is difficult to purify. Early kinetic studies were carried out with microsomal or detergent-solubilized enzyme preparations (*4*−*10*). Although the biosynthetic reactions from FPP to squalene were elucidated in the 1950s and 1960s, it was not until Sasiak and Rilling purified yeast squalene synthase to homogeneity in 1988 that it became clear that both reactions were catalyzed by a single enzyme (*10*).

Analysis of amino acid sequences for squalene synthase provided insights for engineering more soluble variants. Jennings et al. cloned the yeast squalene synthase gene in 1991 (*11*) and suggested that the enzyme consisted of a large cytosolic domain anchored to the endoplasmic reticulum by a single C-terminal transmembrane helix. Subsequently, a soluble and fully active version of recombinant yeast squalene synthase was constructed by deletion of a C-terminal hydrophobic region from the wild-type enzyme (*12*, *13*). *Escherichia coli* clones that express the truncated gene provide a convenient source of soluble enzyme (*12*, *14*).

Scheme 1: Reactions Catalyzed by Squalene Synthase

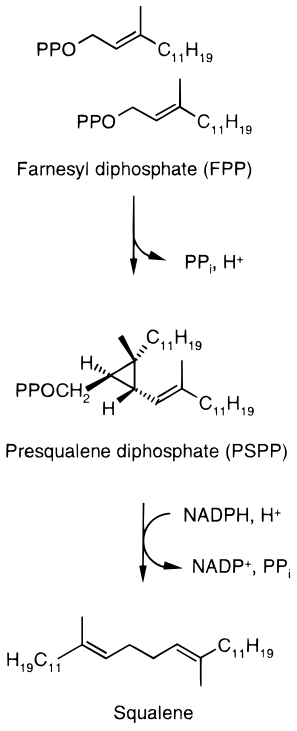


Previous investigators attempted to characterize the chemical and kinetic mechanisms of the two reactions catalyzed by squalene synthase by studying each individually. The enzyme converts FPP to PSPP in the absence of NADPH or NADH and to squalene when incubated with PSPP and

† This research was supported by NIH Grant GM 21328.

* To whom correspondence should be addressed. Phone: (801) 581-6685. Fax: (801) 581-4391. E-mail: poulter@chemistry.utah.edu.

‡ NSF Predoctoral Fellow.

[1] Abbreviations: FPP, E,E-farnesyl diphosphate; PSPP, presqualene diphosphate; βME, 2-mercaptoethanol; EDTA, ethylenediamiine-*N*,*N*,*N*′,*N*′-tetraacetic acid; EGTA, ethylene glycol bis(β-aminoethyl ether)*N*,*N*′-tetraacetic acid; PMSF, phenylmethanesulfonyl fluoride; Mops, 3-(*N*-morpholino)propanesulfonic acid; BSA, bovine serum albumin; HPLC, high-pressure liquid chromatography; IPP, isopentenyl diphosphate; SDS−PAGE, sodium dodecyl sulfate−polyacrylamide gel electrophoresis; DTT, dithiothreitol; TLC, thin-layer chromatography; NADPH, dihydronicotinamide adenine dinucleotide phosphate; $NADP^+$, nicotinamide adenine dinucleotide phosphate; NADH, dihydronicotinamide adenine dinucleotide; $PP_i$, inorganic pyrophosphate; DPM, disintegrations per minute.

10.1021/bi9915014 CCC: $19.00 
Published on Web 01/27/2000

NADPH. An electrophilic cyclopropanation is suspected in the synthesis of PSPP, by analogy with other prenyl transfer enzyme mechanisms, although evidence for the mechanism is sparse (*2*, *15*). In contrast, there is considerable evidence for a cationic cyclopropylcarbinyl rearrangement in the conversion of PSPP to squalene (*2*, *16*, *17*, *18*). Early kinetic experiments were interpreted in favor of a Ping-Pong mechanism for the synthesis of PSPP, followed by an ordered mechanism for the synthesis of squalene from PSPP and NADPH (*6*, *7*). More recent work favored an ordered addition of FPP to two nonequivalent FPP-binding sites during the synthesis of PSPP (*14*). There has been considerable speculation about whether PSPP remains bound to the enzyme during its synthesis from FPP and subsequent conversion to squalene. The speculation includes whether both reactions occur at a single or two separate active sites.

Several observations are pertinent to the kinetic relationship between the first and second reactions. Agnew and Popják reported that FPP inhibited the synthesis of squalene at concentrations above 100 $\mu$M, but not PSPP (*9*). Perhaps as a manifestation of this selective substrate inhibition, the relative amounts of PSPP and squalene produced in other studies appeared to depend on substrate concentrations. In a study by Mookhtiar et al., PSPP and squalene were synthesized at identical rates when [FPP] was below 10 $\mu$M (*14*). However, in studies performed by Muscio et al. (*8*) and Sasiak and Rilling (*10*) using FPP concentrations between 50 and 100 $\mu$M, PSPP accumulated as the first reaction outpaced the second. Agnew and Popják suggested that selective inhibition of squalene synthesis by FPP was evidence for separate catalytic sites and proposed that FPP competed with PSPP at high concentrations by binding nonproductively to the second site (*9*). Several groups found that NADPH accelerated PSPP synthesis, although the cofactor is not required for the first reaction (*5*, *8*−*10*, *12*, *14*). This issue was addressed in a mechanism proposed by Mookhtiar et al. where NADPH adds after formation of PSPP. If dissociation of PSPP from the enzyme•PSPP complex is rate limiting in the absence of NADPH, reduction of PSPP to squalene, which may dissociate more rapidly, would accelerate the synthesis of PSPP from FPP (*14*). There are, however, no reports that bear directly on which step is rate limiting and whether PSPP is released during the normal conversion of FPP to squalene in the presence of NADPH. We now describe steady-state, pre-steady-state, and isotope-trapping experiments that address these issues using soluble recombinant yeast squalene synthase and propose a new mechanism for substrate binding.

## EXPERIMENTAL PROCEDURES

*Preparation of Squalene Synthase.* Truncated recombinant yeast squalene synthase was produced in *E. coli* XA90 and purified essentially as previously described (*12*). Protein concentrations were determined according to the method of Bradford (*19*).

*Preparation of Substrates. (a) Farnesyl Diphosphate.* FPP was synthesized from farnesyl bromide according to the procedure of Davisson et al. (*20*). Concentrations were determined by phosphate analysis using published protocols (*21*, *22*).

*(b) Presqualene Diphosphate.* PSPP was synthesized from FPP. The reaction was carried out at 30 °C in 20 mL of buffer containing 50 mM Mops, pH 7.2, 20 mM $MgCl_2$, and 1 mg/mL BSA. FPP (20 $\mu$mol) was added in five 4 $\mu$mol aliquots at 10 min intervals to give a final concentration of 1 mM FPP. Recombinant squalene synthase (0.7 mg, SA 1.9 $\mu$mol mg$^{-1}$ min$^{-1}$) was added in two equal portions; the first addition initiated the reaction, and the second was added after 60 min, following addition of all of the FPP. Incubation was continued for 3 h with occasional mixing. Insoluble magnesium salts of PSPP formed gradually during the course of the incubation. The turbid solution clarified when the reaction was quenched with 5 mL of 0.5 M EDTA. The solution was extracted three times with 20 mL of 1-butanol, the extracts were combined, and butanol was removed under vacuum. The residue was dissolved in 7 mL of 5:4:1 25 mM $NH_4HCO_3$:acetonitrile:1-butanol to give 6.2 $\mu$mol (62%) of PSPP after HPLC purification (*23*) on a 20 × 300 mm Shodex Asahipak ODP column (Phenomenex). Concentrations were determined by phosphate analysis (*21*, *22*). PSPP was stored dry at −80 °C in small portions of known quantity and was dissolved in buffer containing 5 mM $NH_4HCO_3$, 4% (v/v) Tween-80, and 40% (v/v) 2-propanol shortly before use.

*(c) [1-$^3$H]FPP.* [1-$^3$H]FPP (15−30 mCi/$\mu$mol) was purchased from NEN. This material was acceptable for measuring synthesis of squalene (see below), but gave an unacceptably high background in the proton release assay for PSPP (see below). The background was reduced to acceptable levels by HPLC on a 4.5 × 250 mm Magellan C18 column (Phenomenex) (*23*). [1-$^3$H]FPP was diluted with unlabeled FPP in 25 mM $NH_4HCO_3$ to the desired specific activity and concentration. Stock solutions for kinetic measurements were stored at −80 °C.

*(d) [4,8,12-$^{14}$C]FPP.* Synthesis of [4,8,12-$^{14}$C]FPP from [4-$^{14}$C]IPP was based on a similar procedure for preparing $^{13}$C-labeled FPP, using IPP isomerase and FPP synthase (*24*). Recombinant avian FPP synthase (*25*) was partially purified (*24*) and assayed by the acid lability method (*26*). *Rhodobacter capsulatus* IPP isomerase was purified and assayed as described (*27*).

For synthesis of [4,8,12-$^{14}$C]FPP, the reaction mixture consisted of 0.74 $\mu$mol of [4-$^{14}$C]IPP (54.1 mCi/mmol, NEN), 0.6 mg of IPP isomerase (SA 0.18 $\mu$mol mg$^{-1}$ min$^{-1}$), 0.1 mg of FPP synthase (SA 1.2 $\mu$mol mg$^{-1}$ min$^{-1}$), 10 mM potassium phosphate, pH 7.0, 50 mM KCl, 10 mM $MgCl_2$, 1 mM DTT, and 1 mg/mL BSA in a total volume of 0.3 mL. The reaction was incubated at 30 °C, and synthesis of FPP was monitored at 1−2 h intervals by the acid lability assay. After 5 h the reaction was not complete. The volume was increased to 0.6 mL (maintaining original buffer concentrations), and an additional 0.6 mg of IPP isomerase and 0.1 mg of FPP synthase were added. After 2 h of further incubation, the reaction was quenched by addition of 0.15 mL of 0.5 M EDTA. Proteins were removed by filtration through a Microcon-10 unit (Amicon), and FPP was purified by HPLC as described previously (*23*) on a Prodigy ODS-(3) 4.5 × 250 mm column (Phenomenex). Radiochemical purity was verified by TLC on Diamond LK6DF silica plates (Whatman) developed with 5:3:5 2-propanol:ethyl acetate: concentrated aqueous ammonia and imaged with a Storm 840 phosphorimager (Molecular Dynamics). Radiolabeled FPP was mixed with cold FPP to achieve the desired specific

activity. Stock solutions for kinetic studies were prepared in 25 mM $NH_4HCO_3$ and stored at −80 °C.

*(e) [4,8,12,4′,8′,12′-$^{14}$C]PSPP.* Enzymatic synthesis of [4,8,12,4′,8′,12′-$^{14}$C]PSPP was identical to that of [4,8,12-$^{14}$C]FPP except that 5 $\mu$g of purified squalene synthase (SA 1.2 $\mu$mol mg$^{-1}$ min$^{-1}$) was added to the reaction mixture. The reaction was monitored to minimize the hydrolysis of PSPP by squalene synthase (*16*). When addition of squalene synthase was delayed, $Mg^{2+}$-FPP precipitated and failed to react further. It was essential that FPP synthase and squalene synthase be added simultaneously. In addition, it was necessary to wash the Microcon-10 unit repeatedly with 1-butanol to efficiently recover PSPP. HPLC purification and TLC analysis were as described for FPP. [$^{14}$C]PSPP was stored dry at −80 °C and dissolved in a buffer containing 5 mM $NH_4HCO_3$, 4% (v/v) Tween-80, and 40% (v/v) 2-propanol just before use. Radioactive material was mixed with unlabeled PSPP to achieve the desired specific activity.

*(f) NADPH.* NADPH was purchased from USB and was dissolved in distilled, deionized water or 25 mM $NH_4HCO_3$ immediately before use. Concentrations were determined by UV absorption at 340 nm, using an extinction coefficient of 6200 M$^{-1}$ cm$^{-1}$ (*28*).

*(g) [4B-$^{3}$H]NADPH.* [4B-$^{3}$H]NADPH was prepared by a scaled down version of the protocol for preparing [4B-$^{2}$H]-NADPH (*29*). A 0.3 mL sample of [1-$^{3}$H]D-glucose (0.02 $\mu$mol, 15 Ci/mmol; Sigma) was dried under a stream of argon. The tritiated glucose, 0.05 $\mu$mol of $NADP^+$ (USB), and 110 units of *Leuconostoc mesenteroides* glucose-6-phosphate dehydrogenase (Sigma) were dissolved in 60 $\mu$L of 83 mM potassium phosphate, pH 8.0, and 40 $\mu$L of DMSO, and incubated for 16 h at 23 °C. NADPH was purified by gel filtration (*29*) and analyzed by TLC on Diamond LK6DF silica plates (Whatman) developed with 9.6:0.7:2.2 isobutyric acid:concentrated aqueous ammonia: water and imaged. The radioactivity comigrated with authentic NADPH. [$^{3}$H]NADPH was diluted with unlabeled NADPH immediately before each experiment. The specific activity of the sample was determined by liquid scintillation spectrometry and UV spectroscopy.

*(h) [4B-$^{2}$H]NADPH.* [4B-$^{2}$H]NADPH was prepared and purified as described previously (*29*). Concentrations were determined as described for NADPH.

*Squalene Synthase Assays. (a) Assay for Squalene.* The assay was modified from published protocols (*12*, *18*). Assays contained 50 mM Mops, pH 7.2, 10 mM $MgCl_2$, 1% (v/v) Tween-80, 10% (v/v) 2-propanol, 1 mM DTT, 1 mg/mL BSA, NADPH, FPP (or PSPP), and squalene synthase in a total volume of 200 $\mu$L in glass test tubes unless otherwise specified. Reactions were incubated at 30 °C and were quenched with an equal volume of 1:1 (v/v) 40% aqueous KOH:methanol. Sufficient solid NaCl was added to saturate the mixture, and 2 mL of ligroine containing 0.5% (v/v) squalene was added. The mixture was vortexed vigorously for 30 s. A 1 mL portion of the ligroine layer was applied to a 0.5 × 6 cm alumina column (80−200 mesh, Fisher) packed in a Pasteur pipet and preequilibrated with 2 mL of ligroine containing 0.5% (v/v) squalene. The column was eluted with 5 × 1 mL of toluene containing 0.5% (v/v) squalene. The radioactivity of the eluent was measured in 5 mL of Cytoscint (ICN) or Ecoscint O (National Diagnostics) scintillation cocktail. When greater recoveries of squalene were desired, 1.6 mL (80% recovery of ligroine-soluble radioactivity) of the ligroine extract was applied to the alumina column, although greater care was required during pipetting to not load part of the aqueous layer on to the column.

*(b) Assay for Presqualene Diphosphate (Proton Release Assay).* Assays for proton release were carried out essentially as reported previously (*18*, *30*). The remaining ligroine was carefully removed from the aqueous layer of the squalene assay and discarded. Methanol (2 mL) and a boiling chip were added to the aqueous layer. A U-shaped piece of glass tubing threaded through a rubber stopper was attached to the test tube containing the sample. The test tube was placed in an aluminum block heated to 85 °C, and 1.2−1.5 mL of the contents was distilled into a test tube chilled on ice. A 1 mL portion of the distillate was mixed with 10 mL of Cytoscint cocktail and analyzed for radioactivity. As the distillation proceeded, solvent that distilled later had a slightly higher radioactivity per volume than solvent that distilled earlier. As a result, the small variation between samples in the volume of the distilled solvent contributed a slight nonsystematic error to the assay. However, control experiments demonstrated that 38 ± 2% of exchangeable tritium was consistently recovered. Measured DPMs were divided by 0.38 to correct for the recovery of tritium counts.

*Time Course Measurements.* Time course reactions were carried out at 30 °C using a Kintek rapid mixing machine. Squalene synthase was in 50 mM Mops buffer, pH 7.2, containing 20 mM $MgCl_2$, 4 mg/mL BSA, and 1 mM DTT. [$^{3}$H]FPP and NADPH (when included) were in 50 mM Mops buffer, pH 7.2, containing 2% (v/v) Tween-80, and 20% (v/v) 2-propanol. Upon mixing 24 $\mu$L of enzyme solution with 24 $\mu$L of substrate solution, final concentrations of components other than enzyme, FPP, and NADPH were as follows: 50 mM Mops, pH 7.2, 10 mM $MgCl_2$, 2 mg/mL BSA, 0.5 mM DTT, 1% (v/v) Tween-80, and 10% (v/v) 2-propanol. Reactants were expelled from the rapid mixing machine after the designated reaction time with approximately 100 $\mu$L of buffer [50 mM Mops, pH 7.2, 1% (v/v) Tween-80, and 10% (v/v) 2-propanol] and approximately 175 $\mu$L of quench solution [1:1 (v/v) 40% aqueous KOH: methanol]. Assays for squalene and PSPP were carried out as described above.

*Isotope-Trapping Experiments.* Reactions for isotope trapping were carried out at 30 °C using a Kintek rapid mixing machine. After quenching, the squalene extraction assay was performed, and $^{3}$H and $^{14}$C radioactivities in squalene were measured.

*(a) Trapping of Enzyme [4,8,12-$^{14}$C]FPP Complexes with [4B-$^{3}$H]NADPH.* Typically, 24 $\mu$L of enzyme solution and 24 $\mu$L of [$^{14}$C]FPP solution were mixed and incubated for 1 s, before mixing with 24 $\mu$L of a chase solution containing [4B-$^{3}$H]NADPH and unlabeled FPP. Reactions were quenched after 0.3−40 s upon expulsion with approximately 100 $\mu$L of buffer and approximately 75 $\mu$L of additional chase solution into a test tube containing 300 $\mu$L of a KOH quench solution. The enzyme solution contained 50 mM Mops, pH 7.2, 30 mM $MgCl_2$, 1 mM DTT, 5 mg/mL BSA, and 8−40 $\mu$M squalene synthase. The [$^{14}$C]FPP solution contained 50 mM Mops, pH 7.2, 20% 2-propanol, 2% Tween-80, and 20−120 $\mu$M [4,8,12-$^{14}$C]FPP (3−29 $\mu$Ci/$\mu$mol). Concentrations in the preincubation period, following 1:1 mixing of enzyme

and [$^{14}$C]FPP solutions, were as follows: 4−20 $\mu$M squalene synthase, 10−60 $\mu$M [4,8,12-$^{14}$C]FPP, 50 mM Mops, pH 7.2, 10% 2-propanol, 1% Tween-80, 15 mM $MgCl_2$, 0.5 mM DTT, and 2.5 mg/mL BSA. Chase solution consisted of 1.8 mM [4B-$^3$H]NADPH (6−15 $\mu$Ci/$\mu$mol), 180−280 $\mu$M unlabeled FPP (such that the total concentration of FPP was 100 $\mu$M in the reaction), 50 mM Mops, pH 7.2, 10% 2-propanol, and 1% Tween-80. Reaction concentrations, following 2:1 mixing of preincubated enzyme/[$^{14}$C]FPP and chase solution, were as follows: 2.6−13.3 $\mu$M squalene synthase, 100 $\mu$M FPP, 600 $\mu$M [4B-$^3$H]NADPH, 50 mM Mops, pH 7.2, 10% 2-propanol, 1% Tween-80, 10 mM $MgCl_2$, 0.3 mM DTT, and 1.6 mg/mL BSA.

*(b) Trapping Enzyme [4,8,12,4′,8′,12′-$^{14}$C]PSPP with [4B-$^3$H]NADPH.* Enzyme (24 $\mu$L) and [$^{14}$C]PSPP (24 $\mu$L) solutions were mixed, incubated for 2 s, and combined with 24 $\mu$L of a chase solution containing [4B-$^3$H]NADPH and unlabeled FPP. Reactions were externally quenched after 0.3−65 s, upon being expelled from the rapid mixing machine, as described for the trapping of enzyme [$^{14}$C]FPP complexes. Enzyme solution contained 40 $\mu$M squalene synthase and was otherwise identical to that used for enzyme [4,8,12-$^{14}$C]FPP trapping. [$^{14}$C]PSPP solution contained 100 $\mu$M [4,8,12,4′,8′,12′-$^{14}$C]PSPP (7.4 $\mu$Ci/$\mu$mol), 50 mM Mops, pH 7.2, 20% 2-propanol, and 2% Tween-80. Concentrations in the preincubation period, following 1:1 mixing of enzyme and [$^{14}$C]PSPP solutions, were as follows: 20 $\mu$M squalene synthase, 50 $\mu$M [4,8,12,4′,8′,12′-$^{14}$C]PSPP, 50 mM Mops, pH 7.2, 10% 2-propanol, 1% Tween-80, 15 mM $MgCl_2$, 0.5 mM DTT, and 2.5 mg/mL BSA. The chase solution consisted of 1.8 mM [4B-$^3$H]NADPH (8.6 $\mu$Ci/$\mu$mol), 300 $\mu$M unlabeled FPP, 50 mM Mops, pH 7.2, 10% 2-propanol, and 1% Tween-80. Reaction concentrations, following 2:1 mixing of preincubated enzyme/[$^{14}$C]PSPP and chase solutions, were as follows: 13.3 $\mu$M squalene synthase, 33 $\mu$M [4,8,12,4′,8′,12′-$^{14}$C]PSPP, 100 $\mu$M unlabeled FPP, 600 $\mu$M [4B-$^3$H]NADPH, 50 mM Mops, pH 7.2, 10% 2-propanol, 1% Tween-80, 10 mM $MgCl_2$, 0.3 mM DTT, and 1.6 mg/mL BSA.

*(c) Trapping Enzyme [4B-$^3$H]NADPH with [4,8,12-$^{14}$C]-FPP.* Enzyme/[$^3$H]NADPH (24 $\mu$L) and [$^{14}$C]FPP (24 $\mu$L) were mixed, incubated for 0.1−180 s, and then expelled from the rapid mixing machine with approximately 100 $\mu$L of buffer and approximately 175 $\mu$L of the quench solution. The enzyme/[$^3$H]NADPH solution contained 10 $\mu$M squalene synthase, 300 $\mu$M [4B-$^3$H]NADPH (15 $\mu$Ci/$\mu$mol), 50 mM Mops, pH 7.2, 20 mM $MgCl_2$, 1 mM DTT, and 4 mg/mL BSA. [$^{14}$C]FPP/unlabeled NADPH contained 200 $\mu$M [4,8,-12-$^{14}$C]FPP (2.2 $\mu$Ci/$\mu$mol), 2.7 mM unlabeled NADPH, 50 mM Mops, pH 7.2, 20% 2-propanol, and 2% Tween-80. Reaction concentrations following 1:1 mixing of enzyme/[$^3$H]NADPH and [$^{14}$C]FPP/unlabeled NADPH solutions were as follows: 5 $\mu$M squalene synthase, 100 $\mu$M [4,8,12-$^{14}$C]-FPP, 1.5 mM NADPH, 50 mM Mops, pH 7.2, 10% 2-propanol, 1% Tween-80, 10 mM $MgCl_2$, 0.5 mM DTT, and 2 mg/mL BSA.

*(d) Trapping Enzyme [4B-$^3$H]NADPH with [4,8,12,4′,8′,-12′-$^{14}$C]PSPP.* The experimental procedure was similar to that for trapping of enzyme [$^3$H]NADPH with [$^{14}$C]FPP. The enzyme/[$^3$H]NADPH solution was as above except that the enzyme concentration was 20 $\mu$M, and the specific activity of [4B-$^3$H]NADPH was 52 $\mu$Ci/$\mu$mol. [$^{14}$C]PSPP/unlabeled NADPH solution contained 200 $\mu$M [4,8,12,4′,8′,12′-$^{14}$C]-PSPP (4.2 $\mu$Ci/$\mu$mol), 2.7 mM unlabeled NADPH, 50 mM Mops, pH 7.2, 20% 2-propanol, and 2% Tween-80. Reaction concentrations following 1:1 mixing of enzyme/[$^3$H]NADPH and [$^{14}$C]PSPP/unlabeled NADPH solutions were as follows: 10 $\mu$M squalene synthase, 100 $\mu$M [4,8,12,4′,8′,12′-$^{14}$C]PSPP, 1.5 mM NADPH, 50 mM Mops, pH 7.2, 10% 2-propanol, 1% Tween-80, 10 mM $MgCl_2$, 0.5 mM DTT, and 2 mg/mL BSA.

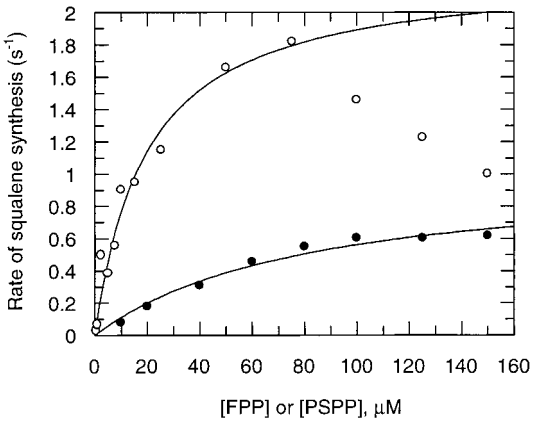


FIGURE 1: Initial rates for squalene synthesis from FPP (○) and PSPP (●), in reactions containing 1 mM NADPH. Reaction mixtures containing NADPH, but not enzyme or isoprenoid substrate, were equilibrated at 30 °C before rapid successive addition of enzyme and [$^3$H]FPP or [$^{14}$C]PSPP. Reactions with FPP (200 $\mu$L total volume) were incubated for 5 min and then quenched. For 0.5−3 $\mu$M FPP, enzyme was 0.11 nM, and [$^3$H]FPP was 818 $\mu$Ci/$\mu$mol; for 5−50 $\mu$M FPP, enzyme was 1.1 nM, and [$^3$H]FPP was 107 $\mu$Ci/$\mu$mol; and for FPP concentrations 75 $\mu$M and higher, enzyme was 11 nM, and [$^3$H]FPP was 8.3 $\mu$Ci/$\mu$mol. Reactions with PSPP ranged in volume from 800 $\mu$L for 10 $\mu$M PSPP to 500 $\mu$L for 175 $\mu$M PSPP and were incubated for 10 min before quenching. Reactions contained 44 pmol of enzyme, and [$^{14}$C]PSPP was 0.2 $\mu$Ci/$\mu$mol. Data for FPP were averages of duplicate determinations, while those for PSPP were single determinations.

## RESULTS

*Squalene Synthase Uses FPP More Efficiently Than PSPP as a Substrate.* The effect of FPP and PSPP concentrations on the initial rate of squalene formation was studied at saturating concentrations of NADPH (1 mM). The results for FPP and PSPP are compared in Figure 1. FPP showed substantial substrate inhibition at higher concentrations. $S_{0.5}^{FPP}$, the half-saturation concentration of FPP for binding to both of its binding sites, was estimated from rates measured for [FPP] < 80 $\mu$M, where substrate inhibition was not obvious, by fitting the data to the Michaelis−Menten equation using Gra-Fit Version 3.0 (Erithacus Software). $V_{max}^{App}$ is an apparent value based on the fit. $S_{0.5}^{FPP} = 19 \pm 4$ $\mu$M, and $V_{max}^{App} = 2.3 \pm 0.2$ s$^{-1}$. Squalene synthase followed normal Michaelis−Menten behavior when PSPP was the substrate; $K_m^{PSPP} = 75 \pm 20$ $\mu$M and $V_{max} = 1.3 \pm 0.2$ s$^{-1}$. The kinetic constants suggest that FPP is preferred over PSPP for squalene at lower [FPP] (*5*) and that PSPP should accumulate as the reaction proceeds if it is released during turnover.

*Rate-Determining Step of the Reaction Sequence Occurs Prior to or Concurrent with PSPP Formation.* Pre-steady-state time course studies were used to identify the rate-determining steps, for the synthesis of PSPP and squalene

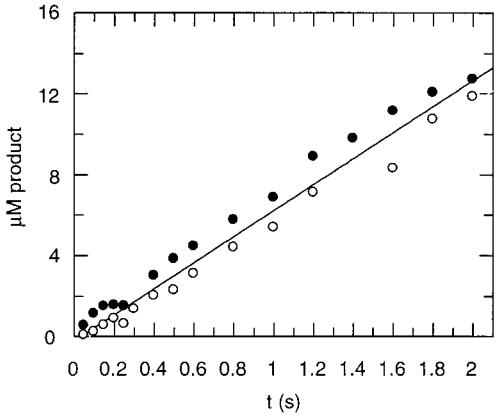


FIGURE 2: Time course for formation of PSPP (●) and squalene (○) from 80 $\mu$M FPP and 1 mM NADPH. The reactions were initiated by combining enzyme and substrate in a rapid mixing machine. The enzyme solution contained 8 $\mu$M squalene synthase, and the substrate solution contained 160 $\mu$M [1-$^3$H]FPP (38 $\mu$Ci/$\mu$mol) and 2 mM NADPH. The final concentrations after 1:1 mixing of enzyme and substrate solutions were 4 $\mu$M squalene synthase, 80 $\mu$M [1-$^3$H]FPP, and 1 mM NADPH; reactions were 0.05−2 s in duration.

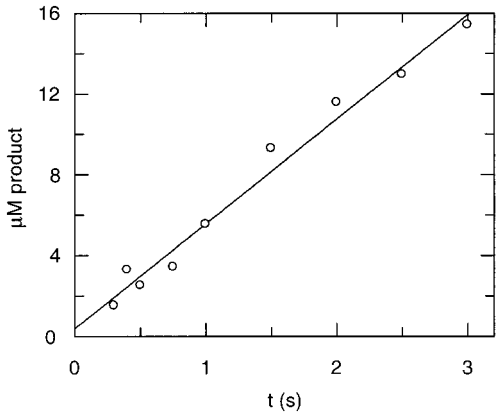


FIGURE 3: Time course for formation of PSPP from 200 $\mu$M FPP, in the absence of NADPH. Reactions were initiated by rapid mixing as described in Figure 2. The enzyme solution contained 8 $\mu$M squalene synthase, and the substrate solution contained 400 $\mu$M FPP (24 $\mu$Ci/$\mu$mol). The final concentrations after 1:1 mixing of enzyme and substrate solutions were 4 $\mu$M squalene synthase and 200 $\mu$M [1-$^3$H]FPP; reactions were 0.2−2.5 s in duration.

from FPP in the presence of NADPH and for the synthesis of PSPP in the absence of NADPH. As shown in Figure 2, a "burst" of PSPP or squalene synthesis was not observed during the first turnover of the enzyme when optimal substrate concentrations were used to achieve a maximal rate of squalene synthesis (80 $\mu$M FPP and 1 mM NADPH). Rates of formation of the two products were identical within the error limits of the assays. Product formation, $k_{cat} = 1.6 \pm 0.1$ s$^{-1}$, was linear for several turnovers when data points from both assays were treated as a single data set or separately, $k_{cat}^{PSPP} = 1.6 \pm 0.1$ s$^{-1}$ and $k_{cat}^{SQ} = 1.50 \pm 0.03$ s$^{-1}$. Similar pre-steady-state kinetic profiles for formation of both PSPP and squalene show that the rate-determining step occurs before PSPP is formed. In addition, the absence of a typical precursor/product profile for PSPP and squalene further supports the suggestion that PSPP does not dissociate from the enzyme during synthesis of squalene from FPP. Data from the corresponding pre-steady-state time course carried out in the absence of NADPH are given in Figure 3. The absence of a burst shows that release of PSPP is not rate limiting. The rate of PSPP synthesis was linear, $k_{cat}^{PSPP} = 1.3 \pm 0.1$ s$^{-1}$. Taken together, these studies demonstrate that product release is not rate limiting, regardless of whether the final product is squalene or PSPP. Thus, the rate-limiting step occurs before or during formation of PSPP and does not change in the absence of NADPH.

*High FPP Concentrations Inhibit Formation of Squalene but Not PSPP.* Substrate inhibition of squalene synthesis at high FPP concentrations has been reported previously (*4*, *7*, *9*, *10*, *12*). An early study suggested that high FPP concentrations inhibit synthesis of squalene but not PSPP (*9*). Since this study included only a few data points at inhibitory FPP concentrations and was performed with crude microsomal enzyme, we decided to reexamine the issue using rapid quench techniques. Time courses were measured at both inhibitory and noninhibitory FPP concentrations, and reactions were assayed for synthesis of both PSPP and squalene. The results are shown in Figure 4. At 100 $\mu$M FPP, neither PSPP nor squalene synthesis was inhibited, and the progress curves were nearly superimposable. However, at 500 $\mu$M

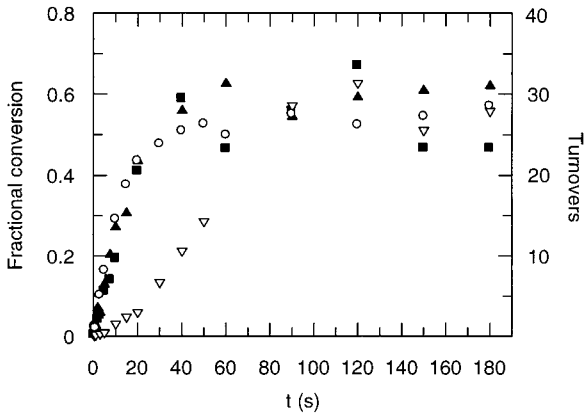


FIGURE 4: Time course for synthesis of PSPP and squalene with 100 and 500 $\mu$M FPP. Data points are represented as follows: PSPP synthesis with 100 $\mu$M FPP (▲), squalene synthesis with 100 $\mu$M FPP (■), PSPP synthesis with 500 $\mu$M FPP (○), squalene synthesis with 500 $\mu$M FPP (▽). All reactions contained 1 mM NADPH. Reactions at low FPP concentrations contained 2 $\mu$M squalene synthase in the enzyme solution and 200 $\mu$M [1-$^3$H]FPP (26 $\mu$Ci/$\mu$mol) and 2 mM NADPH in the substrate solution, for a final concentration after mixing of 1 $\mu$M squalene synthase, 100 $\mu$M [1-$^3$H]FPP, and 1 mM NADPH. Reactions at high FPP concentrations contained 10 $\mu$M squalene synthase in the enzyme solution and 1000 $\mu$M [1-$^3$H]FPP (5.1 $\mu$Ci/$\mu$mol) and 2 mM NADPH in the substrate solution, for a final concentration after mixing of 5 $\mu$M squalene synthase, 500 $\mu$M [1-$^3$H]FPP, and 1 mM NADPH. Time courses were followed with reactions between 0.5 and 180 s in duration at both low and high FPP concentrations. Data points were single determinations.

FPP, there was a marked difference in the rates of PSPP and squalene synthesis. While formation of PSPP synthesis was unimpeded, a substantial and immediate, although transient, inhibition of squalene synthesis was observed.

The rapid recovery of squalene synthesis after 20−30 s may be due to a drop in [FPP] because of precipitation. FPP forms a visible precipitate with magnesium in a time- and concentration-dependent manner (data not shown). The rates observed for PSPP and squalene synthesis just after mixing should reflect the true extent of substrate inhibition at the initial FPP concentrations. However, as the magnesium salts of FPP precipitate, the concentration of soluble FPP will drop, and the rate of the reaction should increase transiently

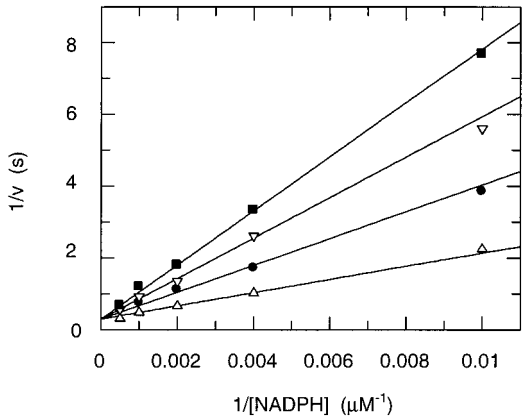


FIGURE 5: Double reciprocal plot of rate of squalene synthesis versus [NADPH], at four inhibitory concentrations of FPP. FPP concentrations are as follows: 200 $\mu$M FPP (△), 300 $\mu$M FPP (●), 400 $\mu$M FPP (▽), and 500 $\mu$M FPP (■). [1-$^3$H]FPP was 2.4 $\mu$Ci/$\mu$mol. The concentration of enzyme was 1.2 $\mu$M, and reactions were incubated for 10 s after addition of FPP before they were quenched. Data points were averages of duplicate determinations.

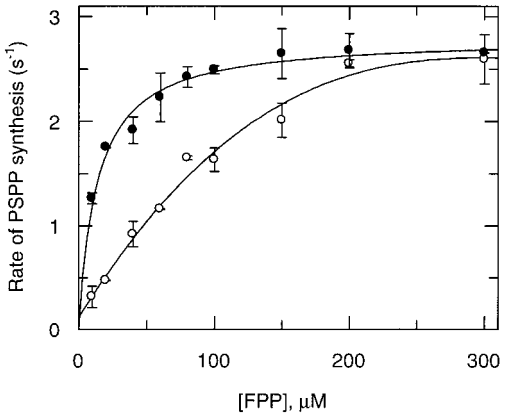


FIGURE 6: Initial rates for PSPP synthesis versus FPP concentration, in the presence (●) or the absence (○) of 1 mM NADPH. FPP concentrations were varied from 10 to 300 $\mu$M, in buffer containing no or 1 mM NADPH. For FPP concentrations between 10 and 80 $\mu$M, [1-$^3$H]FPP (20 $\mu$Ci/$\mu$mol) was incubated with 125 nM enzyme. For [FPP] ≥ 100 $\mu$M, [1-$^3$H]FPP (4.0 $\mu$Ci/$\mu$mol) was incubated with 750 nM enzyme. Reactions were quenched after 10 s, and samples were analyzed with the proton release assay. Data points were averages of duplicate determinations.

as substrate concentrations drop below inhibitory concentrations. Precipitation of FPP might also account for the scatter in the data at longer reaction times and the failure of the reactions to reach completion.

*Substrate Inhibition by FPP is Competitive with NADPH.* To further characterize the mechanism of substrate inhibition by FPP, inhibition studies were conducted where [NADPH] was varied at different inhibitory concentrations of FPP, and reactions were analyzed for squalene formation. Because FPP precipitates in a time- and concentration-dependent manner from the $Mg^{2+}$-containing assay buffer at these concentrations, the most consistent and reproducible results were obtained using shorter reaction times and correspondingly higher concentrations of enzyme. The double reciprocal plot shown in Figure 5 shows competitive inhibition. This is consistent with a binding mechanism where a third molecule of FPP binds to the E·FPP·FPP ternary complex at higher concentrations, blocking formation of an E·FPP·FPP·NADPH complex, but not substantially interfering with the reaction to form PSPP.

*Both High FPP and NADPH Concentrations Stimulate PSPP Formation.* In previous kinetic studies, it was observed that the rate of PSPP synthesis was enhanced by NADPH (*5*, *8*−*10*, *12*, *14*). This phenomenon was usually explained by a rate-limiting dissociation of PSPP from E·FPP·FPP that is circumvented by its immediate conversion to squalene in the intermediate E·PSPP·NADPH complex (*9*, *10*, *14*). However, this explanation is inconsistent with the more comprehensive results presented here. As seen in Figure 3, dissociation of PSPP is not rate limiting, and in the absence of NADPH, the rate-determining step still occurs before PSPP is formed.

An alternative explanation is required for the observed stimulatory effect of NADPH on PSPP synthesis. Since competitive substrate inhibition by FPP at different NADPH concentrations indicates that FPP and NADPH bind to the same form of the enzyme, rates of PSPP formation were measured over a broad range of FPP concentrations with and without NADPH.

The rate of PSPP synthesis was enhanced at high concentrations of FPP in the absence of NADPH, as illustrated in Figure 6. In the presence of 1 mM NADPH, a plot of the rate of PSPP formation versus [FPP] fits a saturation curve with $S_{0.5}^{FPP} = 13 \pm 1$ $\mu$M, similar to the value of 19 $\mu$M observed for squalene formation deduced from steady-state kinetic measurements (see Figure 1). Rates of PSPP synthesis were slower in the absence of NADPH at low FPP concentrations but matched those seen in the presence of NADPH at FPP concentrations ≥ 200 $\mu$M. This observation is consistent with a model where formation of a quaternary complex, either by binding of NADPH or a third molecule of FPP to E·FPP·FPP, stimulates production of PSPP. Mookhtiar et al. observed an increase in the rate of synthesis of PSPP at intermediate (>1 $\mu$M), versus low (0.1−0.5 $\mu$M), FPP concentrations in the absence of NADPH (*14*). They suggested that the acceleration might result from increased competition for the enzyme by FPP, assuming that PSPP release was rate limiting (*14*). Our results suggest a different model where the rate of PSPP formation is stimulated by FPP binding to the E·FPP·FPP complex, even at moderate concentrations of FPP, in the absence of NADPH.

*Hydride Transfer in Squalene Synthesis Displays No Significant Kinetic Isotope Effect.* Quantitative treatment of the data from dual isotope-trapping studies described later require a correction if there is a primary kinetic isotope effect on hydride transfer from NADPH during the reductive rearrangement of PSPP to squalene. The $^1H/^2H$ kinetic isotope effect on hydride transfer to squalene was measured by competition experiments between [4B-$^1$H]NADPH/[4B-$^3$H]NADPH (*31*) and [4B-$^2$H]NADPH/[4B-$^3$H]NADPH, where a H/T isotope effect should exceed a D/T effect as predicted by reduced mass considerations (*32*).

The amount of $^{14}$C-radioactivity in squalene when the reaction goes to completion is

$$^{14}\text{C-DPM}^{(f=1)} = (2.22 \times 10^6 \text{ dpm}/\mu\text{Ci})\text{FPP}_{tot}\,\text{SA}_{FPP}(0.8) \quad (1)$$

where $FPP_{tot}$ is the moles of FPP in the reaction, $SA_{FPP}$ is the specific activity of FPP, and the factor of 0.8 represents

Scheme 2. Trapping Schemes[a]

**a. Binary trappable complex**

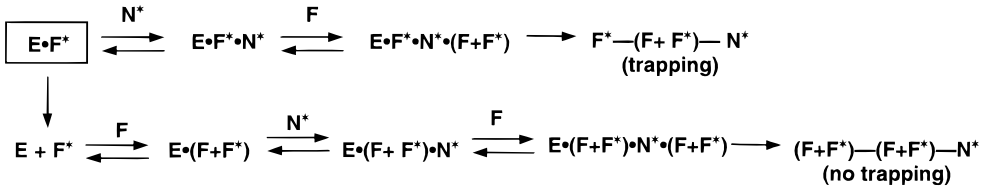


**b. Ternary trappable complex**

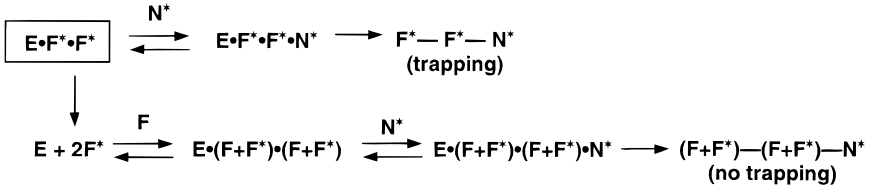


[a] **E** represents the enzyme, **F*** represents [$^{14}$C]FPP, **F** represents cold FPP in the chase solution, **N*** represents [4B-$^{3}$H]NADPH, and squalene is represented as a joining of the three substrates involved in its synthesis, although only the hydride of the involved NADPH is actually present in squalene. (a) Trapping scheme for a binary trappable complex. (b) Trapping scheme for a ternary trappable complex.

the efficiency of squalene recovery in the assay. The fractional completion with respect to FPP for a reaction ($f_{FPP}$) is

$$f_{FPP} = \frac{^{14}\text{C-DPM}_{obs}}{^{14}\text{C-DPM}^{(f=1)}} \quad (2)$$

where $^{14}$C-DPM$_{obs}$ is the $^{14}$C radioactivity observed in the assay.

Since the reactions contained a 5-fold excess of NADPH relative to FPP, and 2 equiv of FPP react with 1 equiv of NADPH, the fractional consumption of NADPH ($f_{NADPH}$) was 10-fold lower than that of FPP, as expressed in eq 3.

$$f_{NADPH} = \frac{f_{FPP}}{10} \quad (3)$$

The specific activity of $^{14}$C in squalene was assumed to be $2S_{FPP}$, since 2 mol of FPP is needed to form a mole of squalene, and the $^{14}$C label was incorporated at remote positions where kinetic isotope effect are negligible. The specific activity of $^{3}$H in the product ($SA_{SQ}$) was calculated using eq 4.

$$SA_{SQ} = 2\left[S_{FPP}\left(\frac{^{3}\text{H-DPM}_{obs}}{^{14}\text{C-DPM}_{obs}}\right)\right] \quad (4)$$

$(V/K)_H/(V/K)_T$ or $(V/K)_D/(V/K)_T$ isotope effects were calculated using eq 5 (*33*) from averages for six reactions at

$$(V/K) = \frac{\log(1-f_{NADPH})}{\log(1 - f_{NADPH}SA_{SQ}/SA_{NADPH})} \quad (5)$$

fractional conversions ($f_{NADPH}$) ranging 0.006−0.03.

The calculated values were $(V/K)_H/(V/K)_T = 1.00 \pm 0.01$ and $(V/K)_D/(V/K)_T = 1.01 \pm 0.01$. We conclude that there was no significant isotope effect on hydride transfer.

*Complexes of Squalene Synthase with FPP Are Trapped with NADPH.* Isotope-trapping experiments used to determine the binding order of FPP and NADPH were patterned after similar studies for FPP synthase (*34*). Preformed complexes between squalene synthase and [$^{14}$C]FPP were chased with a solution containing [$^{3}$H]NADPH and excess unlabeled FPP. If enzyme-bound [$^{14}$C]FPP is trapped by [$^{3}$H]-NADPH, squalene synthesized during the first turnover of the enzyme has a higher $^{14}$C/$^{3}$H ratio than squalene synthesized in subsequent turnovers, after the specific activity of [$^{14}$C]FPP is reduced by dilution with unlabeled substrate. Since squalene synthase converts FPP to PSPP in the absence of NADPH, it was necessary to preassociate enzyme and [$^{14}$C]FPP for only a brief period before the chase solution was added. Quenched samples were assayed for squalene $^{14}$C/$^{3}$H radioactivity.

Equations to calculate to fraction of bound substrate trapped were adapted from a derivation reported by Laskovics and Poulter for FPP synthase (*34*). Two different trapping scenarios were considered for preformed complexes between squalene synthase and FPP. In the most straightforward case, NADPH adds to and traps the ternary E•[$^{14}$C]-FPP•[$^{14}$C]FPP complex. However, if NADPH does not add to the ternary complex, trapping is still possible by ordered addition of NADPH and FPP to the binary E•[$^{14}$C]FPP complex. Equations were derived for each of these possibilities; the case for the binary trappable complex is considered first. Two possible fates for the E•[$^{14}$C]FPP complex following addition of the chase solution are shown in Scheme 2a. The binary complex can be trapped, by successive binding of NADPH and FPP and conversion to squalene, or the complex can dissociate without trapping. The $^{14}$C-radioactivity in squalene as a function of time is

$$^{14}\text{C-DPM}^t = (2.2 \times 10^6\ \text{dpm}/\mu\text{Ci})[(\text{SA}_1 + \text{SA}_2)\text{PE}_{\text{tot}} + 2\text{SA}_2(1 - P)E_{\text{tot}} + (I_t - 1)2\text{SA}_2E_{\text{tot}}] \quad (6a)$$

where $SA_1$ is the specific activity of [$^{14}$C]FPP ($\mu$Ci/$\mu$mol) in the preformed E·[$^{14}$C]FPP complex, $SA_2$ is the specific activity of [$^{14}$C]FPP ($\mu$Ci/$\mu$mol) after mixing with the chase solution containing [$^3$H]NADPH and unlabeled FPP, $E_{tot}$ is the total number of moles of active sites, $P$ is the fractional amount of E·[$^{14}$C]FPP trapped (expressed as a mole fraction of $E_{tot}$), and $I_t$ is the number of turnovers at time $t$. The first two terms in eq 6a represent the $^{14}$C-radioactivity incorporated into squalene from [$^{14}$C]FPP and ([$^{14}$C]FPP + cold FPP), respectively, during the first turnover of the enzyme, and the third term represents the $^{14}$C-radioactivity incorporated into squalene from subsequent turnovers. Upon rearrangement, eq 6a becomes

$$^{14}\text{C-DPM}^t = (2.2 \times 10^6\ \text{dpm}/\mu\text{Ci})[(\text{SA}_1 - \text{SA}_2)P + 2I_tS_2]E_{\text{tot}} \quad (7a)$$

Similarly, the $^3$H-radioactivity incorporated into squalene from [4B-$^3$H]NADPH as a function of time is

$$^{3}\text{H-DPM}^t = (2.2 \times 10^6\ \text{dpm}/\mu\text{Ci})I_t\text{SA}_3E_{\text{tot}} \quad (8)$$

where $SA_3$ is the specific activity of [$^3$H]NADPH ($\mu$Ci/$\mu$mol). Dividing eq 7a by eq 8 gives

$$\frac{^{14}\text{C-DPM}^t}{^{3}\text{H-DPM}^t} = \frac{(\text{SA}_1 - \text{SA}_2)P}{\text{SA}_3I_t} + \frac{2\text{SA}_2}{\text{SA}_3} \quad (9a)$$

where the $^{14}$C/$^3$H ratio in squalene is expressed as a function of the turnover number $I_t$. A plot of $^{14}$C/$^3$H versus the reciprocal of $I_t$ should be linear with a slope proportional to $P$.

For a trappable ternary E·[$^{14}$C]FPP·[$^{14}$C]FPP complex, the equations corresponding to eq 6a, eq 7a, and eq 9a take a slightly different form. The two possible fates for the ternary complex are shown in Scheme 2b. E·[$^{14}$C]FPP·[$^{14}$C]FPP can be trapped by addition of NADPH and converted to squalene, or the complex can dissociate with no trapping. The $^{14}$C-radioactivity incorporated into squalene from [$^{14}$C]FPP as a function of the number of turnovers is

$$^{14}\text{C-DPM}^t = (2.2 \times 10^6\ \text{dpm}/\mu\text{Ci})[2\text{SA}_1\text{PE}_{\text{tot}} + 2\text{SA}_2(1 - P)E_{\text{tot}} + (I_t - 1)2\text{SA}_2E_{\text{tot}}] \quad (6b)$$

As described above for eq 6a, the first two terms represent $^{14}$C-radioactivity incorporated into squalene from [$^{14}$C]FPP and ([$^{14}$C]FPP + cold FPP), respectively, during the first turnover of the enzyme, and the third term represents the $^{14}$C-radioactivity incorporated into squalene during subsequent turnovers. The two scenarios differ in the number of FPP molecules with a specific activity of $SA_1$ that are trapped and incorporated into squalene during the first turnover. For E·[$^{14}$C]FPP, squalene from the first turnover contains only one FPP molecule with a specific activity of $SA_1$, while if E·[$^{14}$C]FPP·[$^{14}$C]FPP is trapped, two molecules of FPP with a specific activity of $SA_1$ are incorporated into squalene. Upon rearrangement, eq 6b becomes

$$^{14}\text{C-DPM}^t = (2.2 \times 10^6\ \text{dpm}/\mu\text{Ci})[(2\text{SA}_1 - 2\text{SA}_2)P + 2I_t\text{SA}_2]E_{\text{tot}} \quad (7b)$$

Dividing eq 7b by eq 8 gives

$$\frac{^{14}\text{C-DPM}^t}{^{3}\text{H-DPM}^t} = \frac{2(\text{SA}_1 - \text{SA}_2)P}{\text{SA}_3I_t} + \frac{2\text{SA}_2}{\text{SA}_3} \quad (9b)$$

Again, a plot of the $^{14}$C/$^3$H ratio in squalene versus the reciprocal of $I_t$ should be linear with a slope proportional to $P$.

Assuming that $E_{tot}$ and $SA_3$ are known, the radioactivity incorporated into squalene from [$^3$H]NADPH in a single turnover is

$$^{3}\text{H-DPM}^{(I=1)} = (2.2 \times 10^6\ \text{dpm}/\mu\text{Ci})\text{SA}_3E_{\text{tot}} \quad (10)$$

Thus, the turnover number at a given time under conditions where the reaction is irreversible is calculated from eq 11

$$I_t = \frac{^{3}\text{H-DPM}^t}{^{3}\text{H-DPM}^{(I=1)}} \quad (11)$$

$P$ can be calculated from the slope of a plot of $^{14}$C-DPM$^t$/$^3$H-DPM$^t$ versus $1/I_t$. The fractional amount of enzyme trapped ($P$), calculated in this manner, is 2-fold higher for E·[$^{14}$C]FPP than for E·[$^{14}$C]FPP·[$^{14}$C]FPP.

Obtaining accurate estimates of $I_t$ for squalene synthase is not straightforward. Calculations of $I_t$ according to eqs 10 and 11 assume that all turnovers lead to squalene. However, we have already shown that under certain conditions squalene synthase can release PSPP prior to formation of squalene. Estimates of $I_t$ based on the amount of tritium incorporated into squalene from [4B-$^3$H]NADPH only count catalytic events resulting in formation of squalene. As a consequence, the fraction of $E_{tot}$ *not* trapped ($1 - P$) also includes any E·[$^{14}$C]FPP·[$^{14}$C]FPP or E·[$^{14}$C]FPP complexes that produce PSPP rather than squalene. Thus, the enzyme may catalyze the formation and release of many molecules of PSPP and still not have undergone turnover all of the way to squalene.

The fraction of squalene synthase that yields squalene in the first turnover can be calculated by correcting $E_{tot}$ for that amount of PSPP that dissociates. At the substrate concentrations used in our trapping experiments where FPP and NADPH were approximately 5-fold higher than their $S_{0.5}$ values, the substrate-binding sites were near saturation. When the initial rate of squalene synthesis in a trapping study was below the experimentally determined maximal rate, we assumed the decrease was due to competing synthesis of PSPP and the enzyme was functioning at its maximal rate. Thus, the moles of enzyme that produce squalene in the first turnover ($E^{\dagger}_{tot}$) is given by

$$E^{\dagger}_{\text{tot}} = \frac{E_{\text{tot}}\upsilon}{V_{\text{max}}} \quad (12)$$

where $\upsilon$ is the observed initial rate of squalene formation in the trapping study and $V_{max}$ is the corresponding maximal rate for the same preparation of enzyme. When $E^{\dagger}_{tot}$ is substituted for $E_{tot}$ in eq 10 and this substitution is propagated

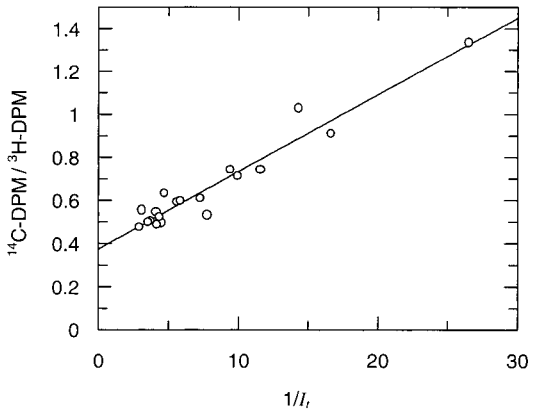


FIGURE 7: Trapping of preformed enzyme·[$^{14}$C]FPP complexes with [$^{3}$H]NADPH. Conditions are described in Experimental Procedures; positive slope indicates trapping.

through eqs 11, 9a, and 9b, eqs 9a and 9b can be rewritten as eqs 13a and 13b,

$$\frac{^{14}\text{C-DPM}^t}{^{3}\text{H-DPM}^t} = \frac{(\text{SA}_1 - \text{SA}_2)P^\dagger}{S_3 I_t^\dagger} + \frac{2\text{SA}_2}{\text{SA}_3}$$

(for a binary trappable complex) (13a)

$$\frac{^{14}\text{C-DPM}^t}{^{3}\text{H-DPM}^t} = \frac{2(\text{SA}_1 - \text{SA}_2)P^\dagger}{\text{SA}_3 I_t^\dagger} + \frac{2\text{SA}_2}{\text{SA}_3}$$

(for a ternary trappable complex) (13b)

where $P^\dagger$ represents the fraction of $E_{tot}^\dagger$ that is trapped and $I_t^\dagger$ is the number of turnovers based on $E_{tot}^\dagger$.

For a series of experiments where the FPP concentration in preassociation with the enzyme is varied, while the concentration of NADPH in the chase solution is held constant, a plot of $P^\dagger$ versus [FPP] should give a "saturation curve" for formation of the trappable complex. $S_{0.5}$ for the curve is the FPP concentration, where half of the enzyme is present as a trappable complex, and the limit of $P^\dagger$ at infinite [FPP] is the efficiency for trapping the preformed complex at a specific [NADPH]. At infinite [NADPH], this limit should approach unity.

Figure 7 shows a plot of $^{14}$C-DPM/$^{3}$H-DPM versus $1/I_t$ for a representative trapping experiment. The positive slope indicates that trapping has occurred. The mole fraction of total enzyme trapped ($P$) in 11 experiments ranged 0.01−0.48 based on trapping E·[$^{14}$C]FPP (eq 9a) or from 0.005 to 0.24 based on trapping E·[$^{14}$C]FPP·[$^{14}$C]FPP (eq 9b). Five of the above experiments were identical except for the concentration of [$^{14}$C]FPP in the preassociation solution. The fraction of enzyme trapped as a mole fraction of enzyme that produced squalene during the first turnover ($P^\dagger$) was calculated from these experiments according to eqs 12, 13a, and 13b. When $P^\dagger$ was plotted versus [$^{14}$C]FPP concentration, a "saturation curve" for formation of the trappable complex was obtained (Figure 8).

Two features of the plot shown in Figure 8 lead us to favor E·[$^{14}$C]FPP·[$^{14}$C]FPP over E·[$^{14}$C]FPP as the trappable species. First, $S_{0.5} = 19 \pm 3\ \mu$M, which is almost identical to $S_{0.5}^{FPP} = 19 \pm 4\ \mu$M observed for squalene synthesis in the steady-state kinetic analysis (see Figure 1). If formation of the trappable complex involved the binding of two molecules

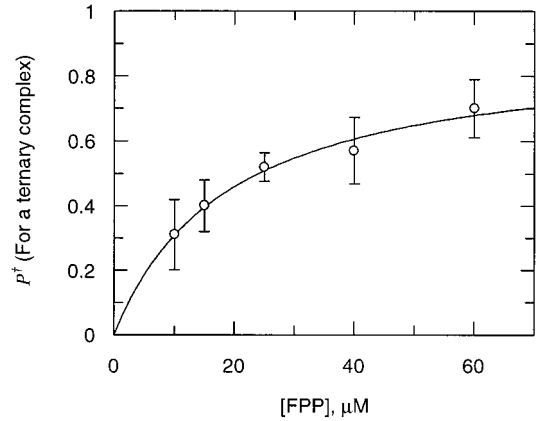


FIGURE 8: Plot of enzyme·FPP complex trapping fraction, corrected for pathway partitioning, versus [FPP] in the complex preformation period. The error bars for $P^\dagger$ reflect errors in the initial rate ($v$) used for calculating $E_{tot}^\dagger$, and the error in the slope used to calculate $P^\dagger$.

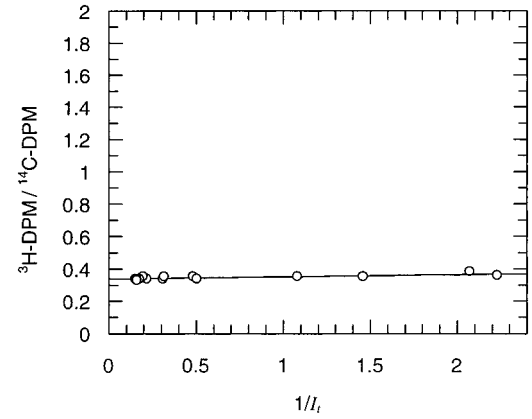


FIGURE 9: Trapping of preformed enzyme·[$^{3}$H]NADPH complexes with [$^{14}$C]FPP. Conditions are described in Experimental Procedures; insignificant slope indicates an absence of trapping.

of FPP, as does squalene synthesis, it is reasonable that the $S_{0.5}$ values for these two phenomena would be similar. Second, the limiting value of $P^\dagger$ predicted from the saturation curve was 0.89 ± 0.06 for E·[$^{14}$C]FPP·[$^{14}$C]FPP, but was twice this value, or approximately 90% higher than the theoretical maximum, for E·[$^{14}$C]FPP. The limiting value of $P^\dagger$ for E·[$^{14}$C]FPP·[$^{14}$C]FPP is consistent with the fixed NADPH concentration of six times the reported $K_m^{NADPH}$ of 100 $\mu$M (*12*) used in these experiments. These results suggest that E·[$^{14}$C]FPP·[$^{14}$C]FPP is the catalytically competent complex that binds NADPH and synthesizes squalene.

*E·NADPH Is Not Trapped with FPP or PSPP.* Several attempts were made to trap E·[$^{3}$H]NADPH with FPP or PSPP. [$^{3}$H]NADPH concentrations exceeded 2 × $K_m^{NADPH}$, and unlabeled NADPH in the chase solution was at least 10-fold higher than the [$^{3}$H]NADPH. This procedure allowed us to detect trapping of as little as 0.2% of the total enzyme. Representative data from experiments with [$^{14}$C]FPP or [$^{14}$C]-PSPP in the chase are plotted in Figures 9 and 10. In neither instance was trapping of E·[$^{3}$H]NADPH observed. These results, taken together with those in the preceding section, indicate that squalene synthase binds two molecules of FPP, followed by NADPH, to produce a catalytically competent E·FPP·FPP·NADPH complex.

*E·PSPP Is Not Trapped with NADPH.* Experiments to detect trapping of E·[$^{14}$C]PSPP were patterned after those

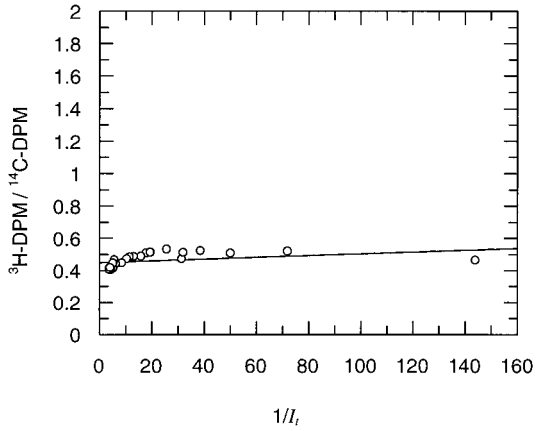


FIGURE 10: Trapping of preformed enzyme·[$^3$H]NADPH complexes with [$^{14}$C]PSPP. Conditions are described in Experimental Procedures; insignificant slope indicates an absence of trapping.

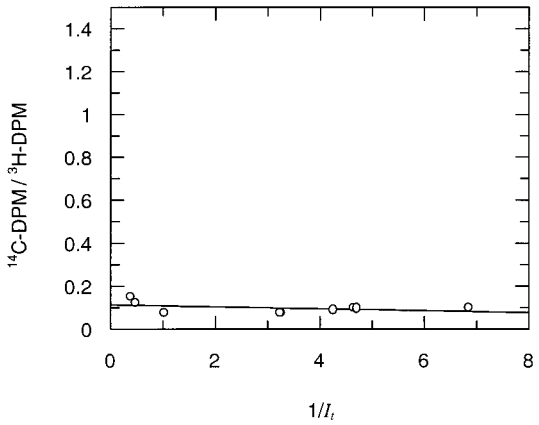


FIGURE 11: Trapping of preformed enzyme·[$^{14}$C]PSPP complexes with [$^3$H]NADPH. Conditions are described in Experimental Procedures; insignificant slope indicates an absence of trapping.

described for enzyme FPP complexes. PSPP was unavailable in the necessary quantities, and unlabeled FPP was used as a replacement in the chase solution. FPP is more efficiently utilized as a substrate by squalene synthase than PSPP and should effectively compete with PSPP after the initial turnover.

A representative set of data is plotted in Figure 11. It is clear from the absence of a positive slope that E·[$^{14}$C]PSPP was not trapped by [$^3$H]NADPH. The $^{14}$C/$^3$H ratio for squalene was consistent with the respective specific activities of [$^{14}$C]PSPP and [$^3$H]NADPH after the addition of chase solution and the relative efficiencies for synthesis of squalene from FPP and PSPP. Our inability to trap E·[$^{14}$C]PSPP is somewhat surprising since PSPP is an intermediate in squalene synthesis from FPP and is converted to squalene when incubated with NADPH. A corrected trapping ($P^\dagger$) of 0.10 would have been *substantially* above the background for this experiment. [PSPP], at 50 $\mu$M, was approximately 0.6 × $K_m$ in the E·[$^{14}$C]PSPP solution, and a premixing time of 2 s should be sufficient for formation of the binary complex. $P^\dagger$ for FPP at [FPP] ≈ $0.6S_{0.5}^{FPP}$ estimated from Figure 8 was 0.35. Thus, E·[$^{14}$C]PSPP is trapped at least 3.5-fold less efficiently than E·[$^{14}$C]FPP·[$^{14}$C]FPP.

*New Binding Mechanism for Squalene Synthase*. We propose the mechanism for substrate binding shown in Scheme 3. Under normal conditions in the presence of FPP and NADPH, squalene synthase binds two molecules of FPP, followed by NADPH. The quaternary E·FPP·FPP·NADPH complex proceeds directly to E·PSPP·NADPH and on to E·squalene·$NADP^+$. At high [FPP], FPP competes with NADPH to form a quaternary E·FPP·FPP·FPP complex that is converted to E·PSPP·FPP, which then dissociates. Formation of a quaternary complex, by the binding of either NADPH *or* FPP, stimulates formation of PSPP. Partitioning between these paths depends on competition between NADPH and FPP for binding to the ternary E·FPP·FPP complex. When [NADPH] is low, free PSPP is formed along with squalene. It is unclear if the tertiary E·FPP·FPP complex is slowly converted to E·PSPP, which then dissociates or if PSPP is formed through a small equilibrium concentration of E·FPP·FPP·FPP.

Since the maximal rates for turnover of E·FPP·FPP·NADPH and E·FPP·FPP·FPP are similar, it is likely that the rate-limiting step is the same for both conversions. A likely candidate is the step described by the rate constant $k_5$ (see Scheme 3), although a rate-limiting conformational change, associated either before or with the chemical step, is possible. The substantial enhancement seen in the rate of PSPP synthesis when NADPH or a third FPP is bound is consistent with a rate-limiting conformational change.

At higher FPP and NADPH concentrations, where FPP and NADPH both stimulate conversion of FPP to PSPP, increasing [FPP] favors synthesis of PSPP, while increasing [NADPH] favors synthesis of squalene. Conversely, increasing [FPP] inhibits squalene synthesis, and increasing [NADPH] inhibits PSPP release by changing the partitioning of E·FPP·FPP between the two paths. The steady-state equations describing this scenario are identical in form to those for alternate substrate inhibition (*35*) as given by

$$v = \frac{V_{max}[\text{NADPH}]}{K_m^{\text{NADPH}}(1 + [\text{FPP}]/K_d^{\text{FPP3}}) + [\text{NADPH}]} \quad (14)$$

$$v' = \frac{V_{max}[\text{FPP}]}{K_d^{\text{FPP3}}(1 + [\text{NADPH}]/K_m^{\text{NADPH}}) + [\text{FPP}]} \quad (15)$$

where $v$ is the rate for synthesis of squalene, $v'$ is the rate for synthesis of free PSPP, $K_m^{NADPH}$ is the Michaelis constant for NADPH, $K_d^{FPP3}$ is the dissociation constant for a third FPP binding to the ternary complex, and $V_{max}$ is the common maximal rate for both pathways. Dividing eq 14 by eq 15 yields eq 16, an expression for the relative rates of the two paths:

$$\frac{v}{v'} = \frac{K_d^{\text{FPP3}}[\text{NADPH}]}{K_m^{\text{NADPH}}[\text{FPP}]} \quad (16)$$

As shown in Figure 6, $v' \approx V_{max}$ at FPP concentrations above 200 $\mu$M in the absence of NADPH. Since the $V_{max}$s are essentially identical for synthesis of PSPP and squalene when measured individually at optimal substrate concentrations, it follows that the total flux through both pathways should equal $V_{max}$ when operating in competition at [FPP] > 200 $\mu$M, as expressed in eq 17:

$$(v + v') \approx V_{max} \quad (17)$$

Thus, $v'$ can be expressed in terms of $v$ and $V_{max}$, by

Scheme 3[a]

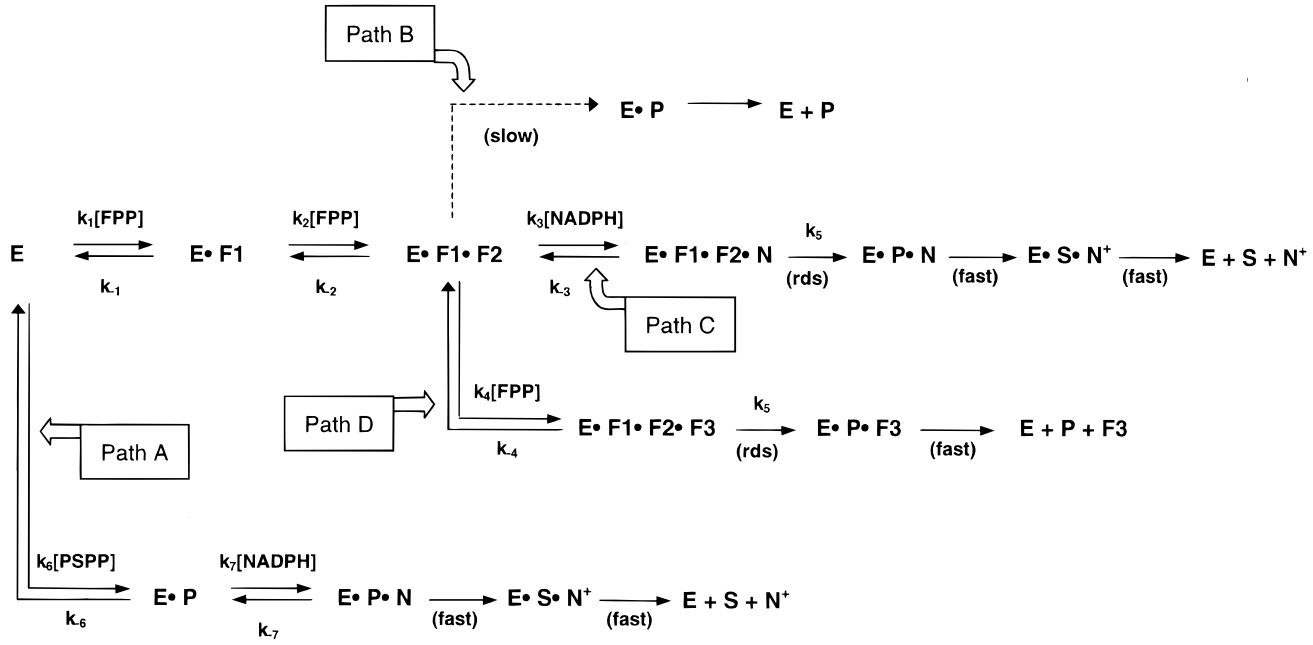


[a] Proposed kinetic mechanism for squalene synthase. **E** represents the enzyme, and **F1**, **F2**, and **F3** refer to the first, second, and third binding molecules of FPP in the ordered sequential mechanism. **N** refers to NADPH, $\mathbf{N}^+$ refers to $NADP^+$, and **P** and **S** correspond to PSPP and squalene, respectively. Pyrophosphate is not illustrated in the scheme, although two molecules of $PP_i$ are formed and released in the synthesis of squalene, because the current investigation did not address the timing of $PP_i$ release in the reaction sequence.

rearrangement of eq 17, and substitution into eq 16 to give

$$\frac{v}{(V_{max} - v)} = \frac{K_d^{FPP3}[NADPH]}{K_m^{NADPH}[FPP]} \quad (18)$$

Rearrangement of eq 18 to a form that describes a double reciprocal plot for $v$ versus [NADPH] gives

$$\frac{1}{v} = \frac{1}{V_{max}} + \frac{K_m^{NADPH}[FPP]}{V_{max}K_d^{FPP3}[NADPH]} \quad (19)$$

The velocity equation described in eq 19 is a simplification of the full rate equation and is only valid for [FPP] > 200 $\mu$M. The slope of a double reciprocal plot of $v$ versus [NADPH] is proportional to [FPP], and a slope replot versus [FPP] has a slope described by the coefficient ($K_m^{NADPH}/V_{max}K_d^{FPP3}$). The value of $V_{max}$ is given by the reciprocal of the $y$-intercept from the double reciprocal plot, and if either $K_m^{NADPH}$ or $K_d^{FPP3}$ is known, the other can be calculated. The $y$-intercept from Figure 5 corresponds to $V_{max} = 3.4\ s^{-1}$. This value for $V_{max}$ is slightly larger than $V_{max}^{App} = 2.3\ s^{-1}$ estimated from the data shown in Figure 1 without correction for substrate inhibition. The slope replot shown in Figure 12 gives $K_m^{NADPH}/V_{max}K_d^{FPP3} = 1.8$ s, and $K_m^{NADPH}/K_d^{FPP3} = 6.2$ for $V_{max} = 3.4\ s^{-1}$.

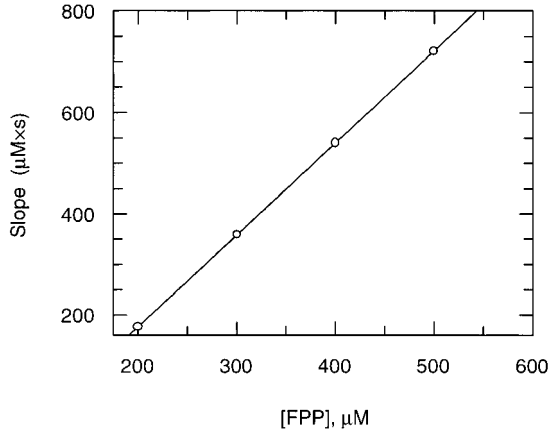


FIGURE 12: Slope replot of inhibition data from Figure 5.

## DISCUSSION

Synthesis of squalene from FPP and NADPH requires two distinct chemical steps—synthesis of PSPP and the reductive rearrangement of PSPP to squalene (*2*). The first step is a prenyl transfer reaction where one of the FPP molecules serves as a prenyl donor and the other as a prenyl acceptor. During synthesis of the cyclopropane ring in PSPP, the diphosphate moiety and a proton are lost from C1 of the prenyl donor as C1 is inserted into the C2−C3 double bond of the second molecule of FPP. The second step, synthesis of squalene from PSPP, involves loss of the diphosphate moiety in PSPP to generate a cyclopropylcarbinyl cation that rearranges and is reduced by NADPH give squalene (*2*, *16*). The chemical mechanism for the second step requires formation of the cyclopropane ring in PSPP before the diphosphate moiety leaves.

When both substrates are present, squalene synthase forms a catalytically competent E·FPP·FPP·NADPH complex that is converted to E·PSPP·NADPH and then to E·squalene·$NADP^+$ without dissociation of PSPP from the enzyme. Synthesis of PSPP is stimulated when NADPH is bound. Our isotope-trapping experiments provide strong evidence that both molecules of FPP bind before NADPH. Mookhtiar et al. (*14*) found that squalene synthase has two distinct FPP binding sites with different affinities for the substrate. They are presumably the prenyl donor and prenyl acceptor sites for the cyclopropanation reaction. Different affinities for the

two FPPs suggest that squalene synthase binds the molecules in a preferred order; however, we cannot distinguish between ordered and random mechanisms or determine which site has the highest affinity for FPP because the *same* molecule is the natural substrate for both sites.

The model we proposed for substrate binding in Scheme 3 has at least three branches (A, C, and D), and perhaps a fourth (B). Each of the paths can become dominant depending on the concentrations of FPP, PSPP, and NADPH. Paths B−D branch from the ternary E·FPP·FPP complex. At low FPP concentrations and either very low or no NADPH, free PSPP can be synthesized slowly from E·FPP·FPP by path B or from a small steady-state concentration of the more reactive E·FPP·FPP·FPP complex by path D. We cannot distinguish between the two possibilities from our data. Enzyme-bound PSPP, whether E·PSPP from path B or E·PSPP·FPP from path D, dissociates much faster than it binds NADPH. However, under steady-state conditions, squalene synthase binds PSPP and NADPH and synthesizes squalene (path A). When no NADPH is present, squalene synthase slowly catalyzes "solvolysis" of PSPP to give a mixture of triterpene hydrocarbons and alcohols (*16*).

At higher NADPH concentrations and low to moderate FPP concentrations, NADPH binds to E·FPP·FPP (path C). Synthesis of PSPP is accelerated, and PSPP is converted to squalene without being released from the enzyme. At higher FPP concentrations, FPP competes with NADPH to form a quaternary E·FPP·FPP·FPP complex (path D). Synthesis of PSPP is accelerated in the E·FPP·FPP·FPP complex. However, squalene synthesis is inhibited, and PSPP accumulates. The binding of either FPP or NADPH to the E·FPP·FPP complex might trigger a conformational change in the enzyme that orients the FPPs in the prenyl donor and acceptor sites in an optimal geometry for reaction. Alternatively, the additional ligand might stabilize a reactive conformation already within the dynamic conformational range of the protein and accelerate PSPP synthesis by shifting the conformational equilibrium.

NADPH and FPP stimulate PSPP formation to similar extents, by binding to the same form of the enzyme. This observation raises the possibility that FPP might also bind to the NADPH-binding site of squalene synthase. Molecular models suggest that FPP can adopt conformations compatible with binding to diphosphate and nicotinamide regions of the NADPH site. A NADPH-binding motif in squalene synthase was located by comparing amino acid sequences with those for phytoene synthase (*36*) and dehydrosqualene synthase (*37*). These enzymes catalyze cyclopropanation and rearrangement reactions similar to those of squalene synthase, except they eventually terminate by elimination of a proton from the final carbocationic intermediate rather than by its reduction (*2*, *16*). Phytoene synthase and dehydrosqualene synthases have substantial sequence similarity with squalene synthase in four conserved regions. A fifth FCAIPQVMA consensus sequence unique to eukaryotic squalene synthases is thought to be the NADPH-binding site. However, motif different than those for NADPH-binding sites commonly found in other enzymes (*38*, *39*).

Although our most informative experiments were performed at high FPP concentrations, these are not the conditions encountered by squalene synthase in vivo. Bruenger and Rilling reported in vivo FPP concentrations between 0.1 and 0.6 $\mu$M in rat and mouse liver tissue (*40*). These FPP concentrations would strongly favor formation of E·FPP·FPP·NADPH and synthesis of squalene without release of the PSPP intermediate. In an in vivo pulse-labeling study with perfused rat liver, Muscio et al. measured the relative rates of free PSPP and squalene synthesis. They found that the amount of PSPP recovered never exceeded 2.4% of that for squalene, and the maximal rate for PSPP synthesis coincided with that for squalene synthesis (*8*). Taken together with our results, it appears that most of the squalene in the liver samples was synthesized directly from FPP without release of PSPP during turnover. If the relative levels of FPP and NADPH in vivo typically favor the direct synthesis of squalene from FPP, there would be no pressure for the evolution of a more discriminating NADPH-binding site in squalene synthase.

The binding mechanism we propose assumes that squalene synthase has a single active site to accommodate both FPP and PSPP. Although there are precedents for enzymes that catalyze two reactions at different sites without releasing intermediates, these systems are large proteins or multisubunit complexes. An example is tryptophan synthase, where indole passes through a tunnel in the interior of the enzyme to travel from one active site to the other (*41*). In contrast, squalene synthase is a relatively small monomer (*12*, *42*). This issue will undoubtedly be resolved soon. A recent report describes the crystallization of a soluble form of recombinant human squalene synthase (*43*), although the X-ray structure is not yet available.

## ACKNOWLEDGMENT

We wish to thank Ms. Suzanne Fernandez and Dr. Frederick Hahn for providing IPP isomerase and Dr. Achilles Leyes for helpful discussions.

## REFERENCES

1. Poulter, C. D., and Rilling, H. C. (1981) in *Biosynthesis of Isoprenoid Compounds* (Porter, J. W., and Spurgeon, S. L., Eds.) Vol. 1, pp 413−441, Wiley, New York.
2. Poulter, C. D. (1991) *Acc. Chem. Res. 23*, 70−77.
3. Stamellos, K. D., Shackelford, J. E., Shechter, I., Jiang, G., Conrad, D., Keller, G.-A., and Krisans, S. K. (1993) *J. Biol. Chem. 268*, 12825−12836.
4. Krishna, G., Whitlock, H. W., Jr., Feldbruegge, D. H., and Porter, J. W. (1966) *Arch. Biochem. Biophys. 114*, 200−215.
5. Shechter, I., and Bloch, K. (1971) *J. Biol. Chem. 246*, 7690−7696.
6. Dugan, R. E., and Porter, J. W. (1972) *Arch. Biochem. Biophys. 152*, 28−35.
7. Beytia, E., Qureshi, A. F., and Porter, J. (1973) *J. Biol. Chem. 248*, 1856−1867.
8. Muscio, F., Carlson, J. P., Kuehl, L., and Rilling, H. C. (1974) *J. Biol. Chem. 249*, 3746−3749.
9. Agnew, W. S., and Popják, G. (1978) *J. Biol. Chem. 253*, 4566−4573.
10. Sasiak, K., and Rilling, H. C. (1988) *Arch. Biochem. Biophys. 260*, 622−627.
11. Jennings, S. M., Tsay, Y. H., Fisch, T. M., and Robinson, G. W. (1991) *Proc. Natl. Acad. Sci. U.S.A. 88*, 6038−6042.
12. Zhang, D., Jennings, S. M., Robinson, G. W., and Poulter, C. D. (1993) *Arch. Biochem. Biophys. 304*, 133−143.
13. LoGrasso, P. V., Soltis, D. A., and Boettcher, B. R. (1993) *Arch. Biochem. Biophys. 307*, 193−199.
14. Mookhtiar, K. A., Kalinowski, S. S., Zhang, D., and Poulter, C. D. (1994) *J. Biol. Chem. 269*, 11201−11207.

15. Gu, P., Ishii, Y., Spencer, T. A., and Shechter, I. (1998) *J. Biol. Chem. 273*, 12515−12525.
16. Jarstfer, M. B., Blagg, B. S. J., Rogers, D. H., and Poulter, C. D. (1996) *J. Am. Chem. Soc. 118*, 13089−13090.
17. Zhang, D., and Poulter, C. D. (1995) *J. Am. Chem. Soc. 117*, 1641−1642.
18. Poulter, C. D., Capson, T. L., Thompson, M. D., and Bard, R. S. (1989) *J. Am. Chem. Soc. 111*, 3734−3739.
19. Bradford, M. M. (1976) *Anal. Biochem. 72*, 248−254.
20. Davisson, V. J., Woodside, A. B., Neal, T. R., Stremler, K. E., Muehlbacher, M., and Poulter, C. D. (1986) *J. Org. Chem. 51*, 4768−4779.
21. Cassidy, P. B., Dolence, J. M., and Poulter, C. D. (1995) *Methods Enzymol. 250*, 30−43.
22. Lanzetta, P. A., Alvarez, L. J., Reinach, P. S., and Candia, O. A. (1979) *Anal. Biochem. 100*, 95−97.
23. Zhang, D., and Poulter, C. D. (1993) *Anal. Biochem. 213*, 356−361.
24. Christensen, D. J., and Poulter, C. D. (1994) *Bioorg. Med. Chem. 2*, 631−637.
25. Tarshis, L. C., Yan, M., Poulter, C. D., and Sacchettini, J. C. (1994) *Biochemistry 33*, 10871−10877.
26. Rilling, H. C. (1985) *Methods Enzymol. 110*, 145−152.
27. Hahn, F. M., Baker, J. A., and Poulter, C. D. (1996) *J. Bacteriol. 178*, 619−624.
28. Malcolm, A. D. B. (1980) *Methods Enzymol. 66*, 8−11.
29. Viola, R. E., Cook, P. F., and Cleland, W. W. (1979) *Anal. Biochem. 96*, 334−340.
30. Kuswik-Rabiega, G., and Rilling, H. C. (1987) *J. Biol. Chem. 262*, 1505−1509.
31. Popják, G., Schroepfer, G., and Cornforth, J. W. (1961/62) *Biochem. Biophys. Res. Commun. 6*, 438−442.
32. Swain, C. G., Stivers, E. C., Reuwer, J. F., Jr., and Schaad, L. J. (1958) *J. Am. Chem. Soc. 80*, 5885−5893.
33. Cleland, W. W. (1982) *CRC Crit. Rev. Biochem. 13*, 385−428.
34. Laskovics, F. M., and Poulter, C. D. (1981) *Biochemistry 20*, 1893−1901.
35. Cornish-Bowden, A. (1995) *Fundamentals of Enzyme Kinetics*, pp 105−108, Portland Press, London.
36. McKenzie, T. L., Jiang, G., Straubhaar, J. R., Conrad, D. G., and Shechter, I. (1992) *J. Biol. Chem. 267*, 21368−21374.
37. Wieland, B., Feil, C., Gloria-Maercker, E., Thumm, G., Lechner, M., Bravo, J.-M., Poralla, K., and Götz, F. (1994) *J. Bacteriol. 176*, 7719−7726.
38. Bellamacina, C. R. (1996) *FASEB J. 10*, 1257−1269.
39. Lesk, A. M. (1995) *Curr. Opin. Struct. Biol. 5*, 775−783.
40. Bruenger, E., and Rilling, H. C. (1988) *Anal. Biochem. 173*, 321−327.
41. Hyde, C. C., Ahmed, S. A., Padlan, E. A., Miles, E. W., and Davies, D. R. (1988) *J. Biol. Chem. 263*, 17857−17871.
42. Shechter, I., Klinger, E., Rucker, M. L., Engstrom, R. G., Spirito, J. A., Islam, M., A., Boettcher, B. R., and Weinstein, D. B. (1992) *J. Biol. Chem. 267*, 8628−8635.
43. Thompson, J. F., Danley, D. E., Mazzalupo, S., Milos, P. M., Lira, M. E., and Harwood, H. J., Jr. (1998) *Arch. Biochem. Biophys. 350*, 283−290.

BI9915014